NASA TECHNICAL MEMORANDUM

NASA TM X-64934

AN ANALYSIS OF THE DAHL FRICTION MODEL AND ITS EFFECT ON A CMG GIMBAL RATE CONTROLLER

By Gerald S. Nurre
Systems Dynamics Laboratory

November 1974

NASA

George C. Marshall Space Flight Center
Marshall Space Flight Center, Alabama

TECHNICAL REPORT STANDARD TITLE PAGE

1. REPORT NO.	2. GOVERNMENT ACCESSION NO.	3. RECIPIENT'S CATALOG NO.
NASA TM X-64934		

4. TITLE AND SUBTITLE	5. REPORT DATE
An Analysis of the Dahl Friction Model and its Effect on a CMG Gimbal Rate Controller	November 1974
	6. PERFORMING ORGANIZATION CODE
7. AUTHOR(S) Gerald S. Nurre	8. PERFORMING ORGANIZATION REPORT #
9. PERFORMING ORGANIZATION NAME AND ADDRESS George C. Marshall Space Flight Center Marshall Space Flight Center, Alabama 35812	10. WORK UNIT NO.
	11. CONTRACT OR GRANT NO.
	13. TYPE OF REPORT & PERIOD COVERED Technical Memorandum
12. SPONSORING AGENCY NAME AND ADDRESS National Aeronautics and Space Administration Washington, D.C. 20546	14. SPONSORING AGENCY CODE

15. SUPPLEMENTARY NOTES

Prepared by Systems Dynamics Laboratory, Science and Engineering

16. ABSTRACT

Recent interest in fine pointing control systems for large orbiting astronomical telescopes has stimulated investigations into the low level torquing characteristics of medium size control moment gyros. The most significant phenomenon that limits the linearity and response at low torque levels is frictional torque in the gimbal pivot. Recent measurements of frictional torque in ball bearings have shown that a stiction-friction characteristic is not a valid model, as was previously thought, but that a more accurate representation is one developed by Dahl. This report presents an explanation of the Dahl friction model and shows, by analytical development, some of its characteristics. The last section of the report shows how friction, represented by the Dahl model, affects the response of a typical gimbal rate control system.

17. KEY WORDS	18. DISTRIBUTION STATEMENT
	Unclassified-unlimited

19. SECURITY CLASSIF. (of this report)	20. SECURITY CLASSIF. (of this page)	21. NO. OF PAGES	22. PRICE
Unclassified	Unclassified	28	NTIS

TABLE OF CONTENTS

LIST OF ILLUSTRATIONS

TECHNICAL MEMORANDUM X-64934

AN ANALYSIS OF THE DAHL FRICTION MODEL AND ITS EFFECT ON A CMG GIMBAL RATE CONTROLLER

I. INTRODUCTION

Recent design work on the fine pointing control system for the Large Space Telescope (LST) has generated a keen interest in the low level torquing characteristics of momentum exchange devices, particularly medium size control moment gyros (CMGs). This attention to CMG actuators stems from the desire to find a single actuator that is adequate for all pointing and maneuver modes of the LST. The definition of low level torquing for the purposes herein is that level of torque resolution required to point the LST to ~ 0.001 arc sec, or approximately 0.01 N-m for a control system natural frequency of 1 Hz. The difficulty in achieving this torque resolution becomes apparent when one calculates the associated gimbal rates. For a 200 N-m-s CMG, as an example, the gimbal must be accurately processed at a rate of 5×10^{-5} rad/s, an angular rate nearly an order of magnitude lower than that of the hour hand of a clock. The problems in building a CMG and its gimbal control system for good low signal performance are primarily caused by frictional torques in the gimbal pivots. Frictional torques in bearings and brushes generally exhibit a nonlinear characteristic at small angular velocities and, consequently, complicate gimbal rate control for small rates about zero.

The precise nature of the frictional mechanism is the subject of some controversy. Since applications that required such extremely low torque levels were nonexistent until recently, only a small amount of information on the subject, either theoretical or experimental, has been published. Consequently, the classical stiction characteristic was used in the initial modeling work. This characteristic, of course, made the medium size CMG undesirable as an actuator for a fine pointing system, and it was not long before the validity of the stiction model began to be questioned. Based on investigations by Dahl[*] and some recent experimental work at Sperry Flight Systems in Phoenix, Arizona,

[*]Dahl, P. R.: A Solid Friction Model. Aerospace Report No. TOR-0158 (3107-18)-1, May 1968.

it is now generally felt that the frictional torque in a gimbal pivot is not at all characterized by the classical stiction model but is more closely represented by a nonlinear spring, with torque being a function of the gimbal displacement. In his report Dahl discusses the various mechanisms for frictional forces arising from various surface conditions in both rolling and rubbing contact. Special emphasis is given to the model for friction in ball bearings, including experimental data which show close agreement with the analytical model. While this agreement in itself lends strong support to the validity of the model, Dahl's representation also seems to incorporate all the phenomena that one might intuitively consider essential to the friction mechanism.

The objective of this document is to extend the interpretation of what the Dahl model does; nothing new is added to the basic theory. There is a section that describes the model and another one, entitled Analytical Results, wherein some interesting dynamical characteristics become apparent as the result of equation manipulations. Another section gives the results of a digital simulation of the equations of motion for rotating mass supported by a roller bearing pivot and influenced only by frictional torque. The last section indicates how frictional torques affect the design of a gimbal rate control system.

II. DESCRIPTION OF THE SQUARE LAW FRICTION MODEL

If $T_f(\theta)$ is defined as the frictional torque, its time derivative can be written as

$$\frac{dT_f}{dt} = \frac{dT_f}{d\theta} \frac{d\theta}{dt} \quad , \tag{1}$$

where θ is the shaft angular displacement. If, then, one can define the function $dT_f/d\theta$ for a given bearing pivot, the frictional torque can be computed. It is apparent, then, that the choice of $dT_f/d\theta$ determines the model. Dahl has postulated the following form for this function:

$$\frac{dT_f}{d\theta} = \gamma \left(T_f \frac{\dot{\theta}}{|\dot{\theta}|} - T_{f0} \right)^2 \quad , \tag{2}$$

the reasonableness of which is supported by experimental data. A block diagram representing equations (1) and (2) is shown in Figure 1. T_{f0} is the maximum frictional torque that can occur and is equivalent to what is commonly termed running friction.

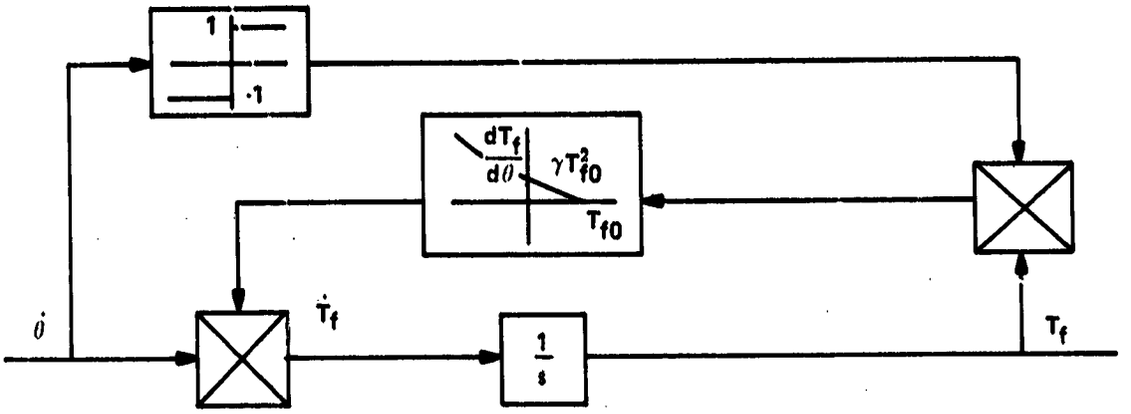

Figure 1. Dahl friction model for ball bearings.

To show the operation of the model, one should determine what happens within the block diagram as the input, $\dot{\theta}$, is varied. It is important to note, first of all, that $dT_f/d\theta$, the output of the square law block, is always positive. Assume that initially all variables are zero, then $\dot{\theta}$ goes positive. Since, for $T_f = 0$, $dT_f/d\theta = \gamma T_{f0}^2$, $\dot{T}_f$ will have a finite positive value and T_f will begin to increase. Because $\dot{\theta}$ is positive the switch is in the positive position; and as T_f increases, $dT_f/d\theta$ becomes smaller. This process continues until $T_f = T_{f0}$ when $dT_f/d\theta = 0$ and $\dot{T} = 0$ so that T_f can no longer increase. If $\dot{\theta}$ becomes negative, the input to the square law block changes sign and, at the instant $\dot{\theta}$ goes negative, $dT_f/d\theta$ jumps from zero to $-\gamma T_{f0}^2$. Thus, $\dot{T}_f$ is negative and the integrator begins integrating down from T_{f0}. It is interesting to note at this point that the frictional torque is in a direction to increase the angular velocity in the negative direction; or colloquially, the friction torque is aiding the motion. This kind of phenomenom is generally not associated with frictional torques; and, if one defines friction as an energy loss mechanism, then it is obvious that the Dahl model incorporates more than energy loss in the pivot. The integrator then continues to integrate from T_{f0} to $-T_{f0}$.

In his report Dahl indicates that T_f has some randomness associated with it due to the nonuniformity of the two contacting surfaces and he has shown how this might be incorporated into the model. This part of the model, however, is not considered in this report.

III. ANALYTICAL CONSIDERATIONS

In the case of a mass free to turn in a pivot and influenced by frictional torques, the equations defining its motion are:

$$I\ddot{\theta} = -T_f \tag{3}$$

and

$$\dot{T}_f = \gamma\left(T_f \frac{\dot{\theta}}{|\dot{\theta}|} - T_{f0}\right)^2 \dot{\theta} \quad , \tag{4}$$

where I is the moment of inertia of the rotating mass about the pivot axis.

Now, consider small motions about the equilibrium point, $T = \dot{\theta} = 0$, so that the equations can be linearized about this point. If the square function on the right-hand side of equation (4) is expanded in a Taylor series, all terms except the first are either zero or second order, and equation (4) reduces to

$$\dot{T}_f = \gamma T_{f0}^2 \dot{\theta} \quad ,$$

which is directly integrable. Thus, equation (3) becomes

$$I\ddot{\theta} + \gamma T_{f0}^2 \theta = 0 \quad , \tag{5}$$

the equation for a linear oscillator with $\gamma' T_{f0}^2$ being the spring rate and natural frequency ω given as

$$\omega^2 = \frac{\gamma' T_{f0}^2}{I} \quad . \tag{6}$$

Hence, to first order, the friction model behaves as an oscillatory second order system with no damping. The absence of a damping term in the linearized equations does not, however, preclude the possibility of asymptotic stability.

It is also of interest to compute T_f as a function of $\dot{\theta}$ and θ where $\dot{\theta} = A \sin \omega_0 t$. Equation (4) can then be integrated in the form

$$\int_{-T_{f_i}}^{T_f} \frac{dT_f}{\gamma \left| T_f - T_{f0} \right|^2} = \int_0^t A \sin \omega_0 t \, dt \tag{7}$$

for $0 \leq \omega_0 t \leq \pi$. Integration of equation (7) gives

$$\frac{T_f}{T_{f0}} = \frac{T_{f0}\gamma \frac{A}{\omega_0} (1 - \cos \omega_0 t) - \frac{\frac{T_{f_i}}{T_{f0}}}{\frac{T_{f_i}}{T_{f0}} + 1}}{\frac{1}{\frac{T_{f_i}}{T_{f0}} + 1} + T_{f0}\gamma \frac{A}{\omega_0} (1 - \cos \omega_0 t)} \quad . \tag{8}$$

The proper value of T_{f_i} for a given A and ω_0 can be found from equation (8) from the condition that $T_f = T_{f_i}$ for $\omega_0 t = \pi$, and the ratio T_{f_i} / T_{f0} has the

form

$$\frac{T_f}{T_{f0}} = -\frac{1}{2T_{f0}\gamma\frac{A}{\omega_0}} + \left[\left(\frac{1}{2T_{f0}\gamma\frac{A}{\omega_0}}\right)^2 + 1\right]^{1/2} \quad . \tag{9}$$

Equation (8) has been plotted as a function of $\dot{\theta}$ and θ in Figures 2 and 3. The angular velocity, $\dot{\theta}$, is a sinusoidal function with a constant amplitude $A = 0.002$ rad/s and ω_0 is varied as a parameter.

These curves, plotted from simulation results, appear in Dahl's report, and he makes the observation that as ω_0 decreases, the shapes of the T_f versus $\dot{\theta}$ curves approach the form of the classical stiction characteristic. This can be seen from equation (8), since as $\omega_0 \to 0$, $T_f/T_{f0} \to 1$ for an arbitrary value of t. On the other hand, as ω_0 increases, the curves become more elliptical in shape. This is indicative of the fact, for $T_f \ll 1$, T_f is a linear function of θ as shown in equations (4) and (5) which will produce an ellipse. Likewise the curves of T_f versus θ approach a straight line through the origin.

The quantity, $1/\gamma T_{f0}$, has the unit of rad and can be interpreted as a characteristic angle for the friction model. The relative size of A/ω_0, the amplitude of the angular motion, with respect to the characteristic angle determines the shape of the curves in Figures 2 and 3. It can be shown, for instance, that the two inflection points in the graphs for small ω_0's disappear for $T_{f0}\gamma\,(A/\omega_0) \cong 2$. Hence, the shapes of the curves change most significantly for amplitudes that are approximately twice the characteristic angle.

IV. SIMULATION RESULTS

In order to verify the analytical results of the previous section, a digital simulation was developed for the gimbal control system depicted in Figure 4. The equations of motion for this system are the following:

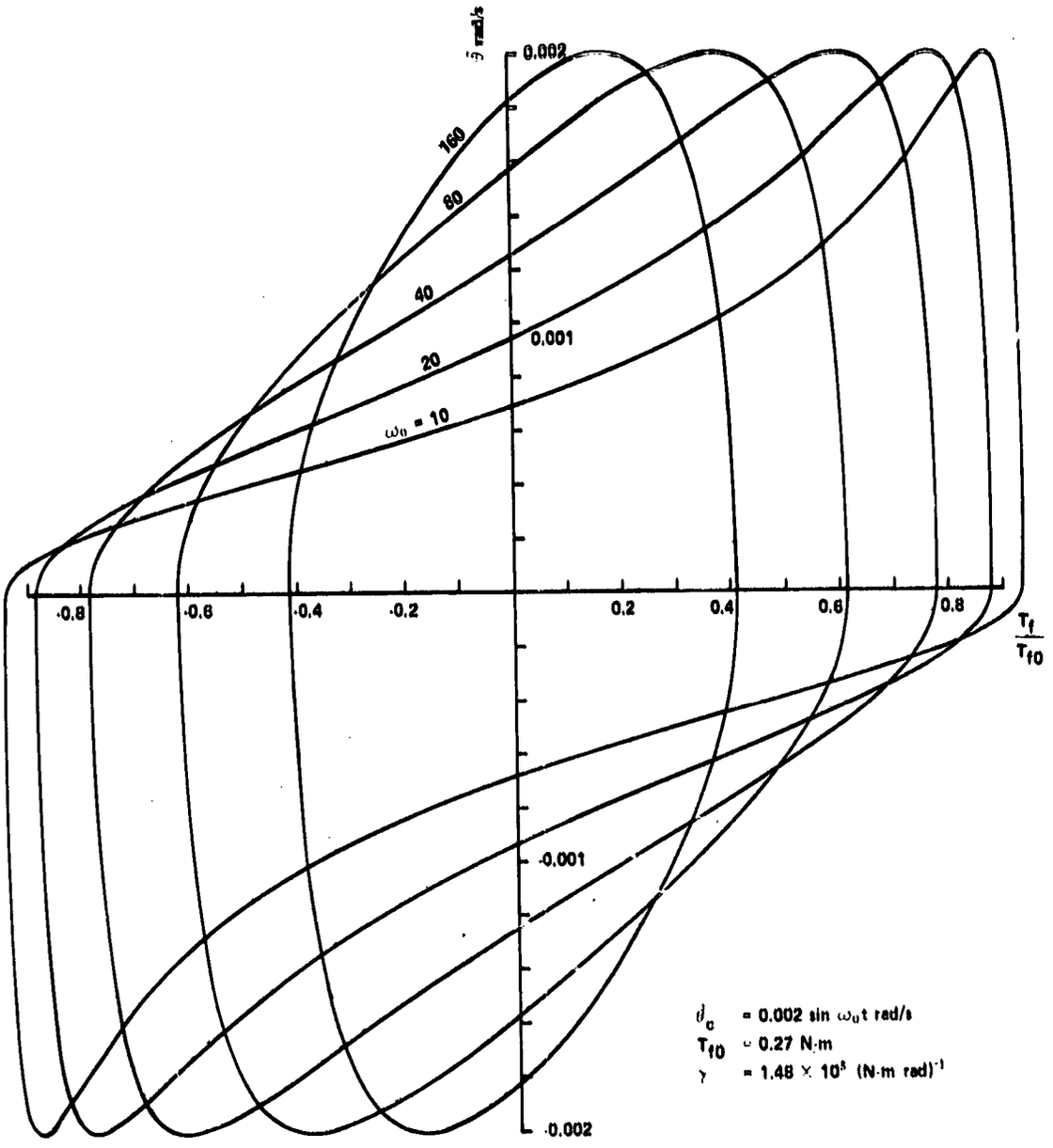

Figure 2. $\dot{\theta}$ versus T_f.

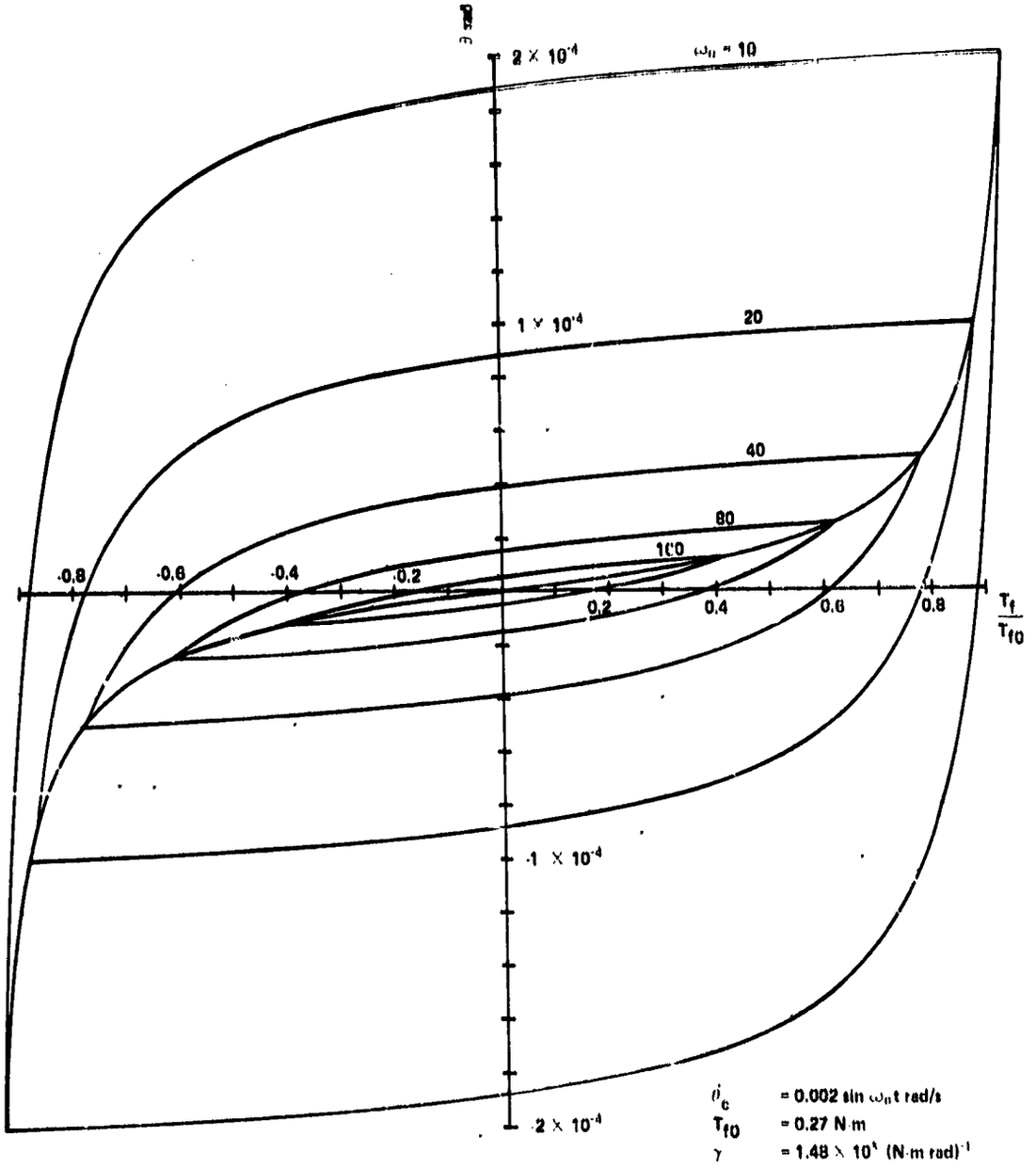

Figure 3. $\dot{\theta}$ versus T_f.

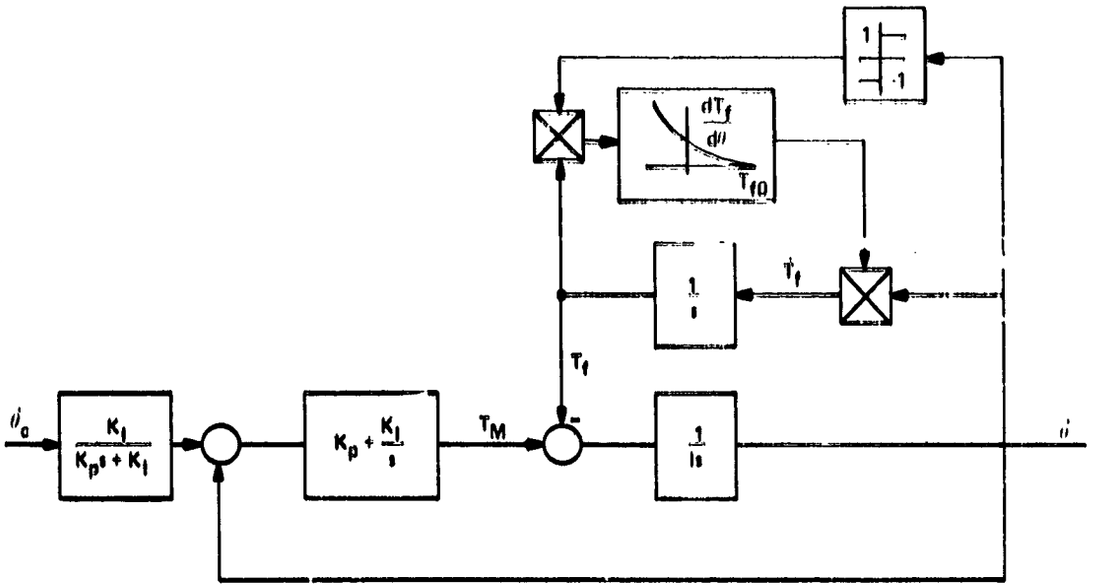

Figure 4. Gimbal rate controller.

$$I\ddot{\theta} = K_p(\dot{\theta}_1 - \dot{\theta}) + K_I(\theta_1 - \theta) - T_f \quad , \tag{10}$$

$$K_p\ddot{\theta}_1 = K_I(\theta_c - \dot{\theta}_1) \quad , \tag{11}$$

and

$$T_f = \gamma\left(T_f \frac{\dot{\theta}}{|\dot{\theta}|} - T_{f0}\right)^2 \dot{\theta} \quad , \tag{12}$$

where I is the effective inertia of the gimbal, K_p and K_I are control system gains, and $\dot{\theta}_c$ is the commanded gimbal rate.

Since initially interest lies in the dynamics due to frictional torques alone, K_p and K_I are set equal to zero. If, then, the rotor is given an initial velocity, it should come to rest under the influence of the frictional torque.

The motion during this time will indicate the general characteristics of the friction model. Figure 5 shows results for an initial $\dot{\theta} = 0.002$ rad/s, and $T_{f0} = 0.0424$ N-m, and $\gamma = 0.85 \times 10^4$ (N-m rad)$^{-1}$; these values of T_{f0} and γ were measured experimentally by Dahl. The inertia, I, was chosen as 5 slug ft^2 which is typical of the effective gimbal inertia of a medium size CMG. Figure 5 shows that for the first quarter of a second, until $\dot{\theta}$ changes sign, $T_f = T_{f0}$. The motion thereafter is similar to that of an underdamped second order system. The period of the oscillatory motion taken from Figure 5 is 3.6 seconds while that computed from equation (6) is 3.65 seconds. Thus, the spring mechanism is evident. It is also noteworthy that as the amplitudes become smaller, the damping decreases, as was found above.

Figure 6 shows similar results for a case with $T_{f0} = 0.27$ N-m and $\gamma = 1.48 \times 10^5$ (N-m rad)$^{-1}$. These values are the result of fitting some experimental data taken on a CMG pivot. These numbers have increased the natural frequency considerably with the measured period equal to 0.138 second and that calculated from equation (4) 0.135 second. If one compares the plots of $\dot{\theta}$ and T_f in Figures 5 and 6, it appears that the two variables are in phase and that T_f is sinusoidal in nature. However, a closer look at T_f subsequent to the times when $\dot{\theta}$ is changing sign indicates that T_f decreases more rapidly than it would if it were a true sine wave. This is due to the switching from a low to a higher gain in the friction model and has the effect of producing damping. As the amplitude decreases, this effect is seen to diminish, since the change in gain at the switching instant becomes less and less.

The characteristics shown in Figures 2 and 3 were verified by commanding a sinusoidal input for $\dot{\theta}_c$ through the control system with $K_I = 10^4$ and $K_p = 280$. The results compare well with those calculated in the previous section.

V. THE EFFECT OF THE FRICTION MODEL ON THE GIMBAL RATE CONTROL SYSTEM

If gimbal pivot friction is neglected, the gimbal rate controller is given by equations (10) and (11) with $T_f = 0$. The natural frequency, ω_c, and damping factor, ζ, for the controller are given by

$$\omega_c = \frac{K_I}{I}$$

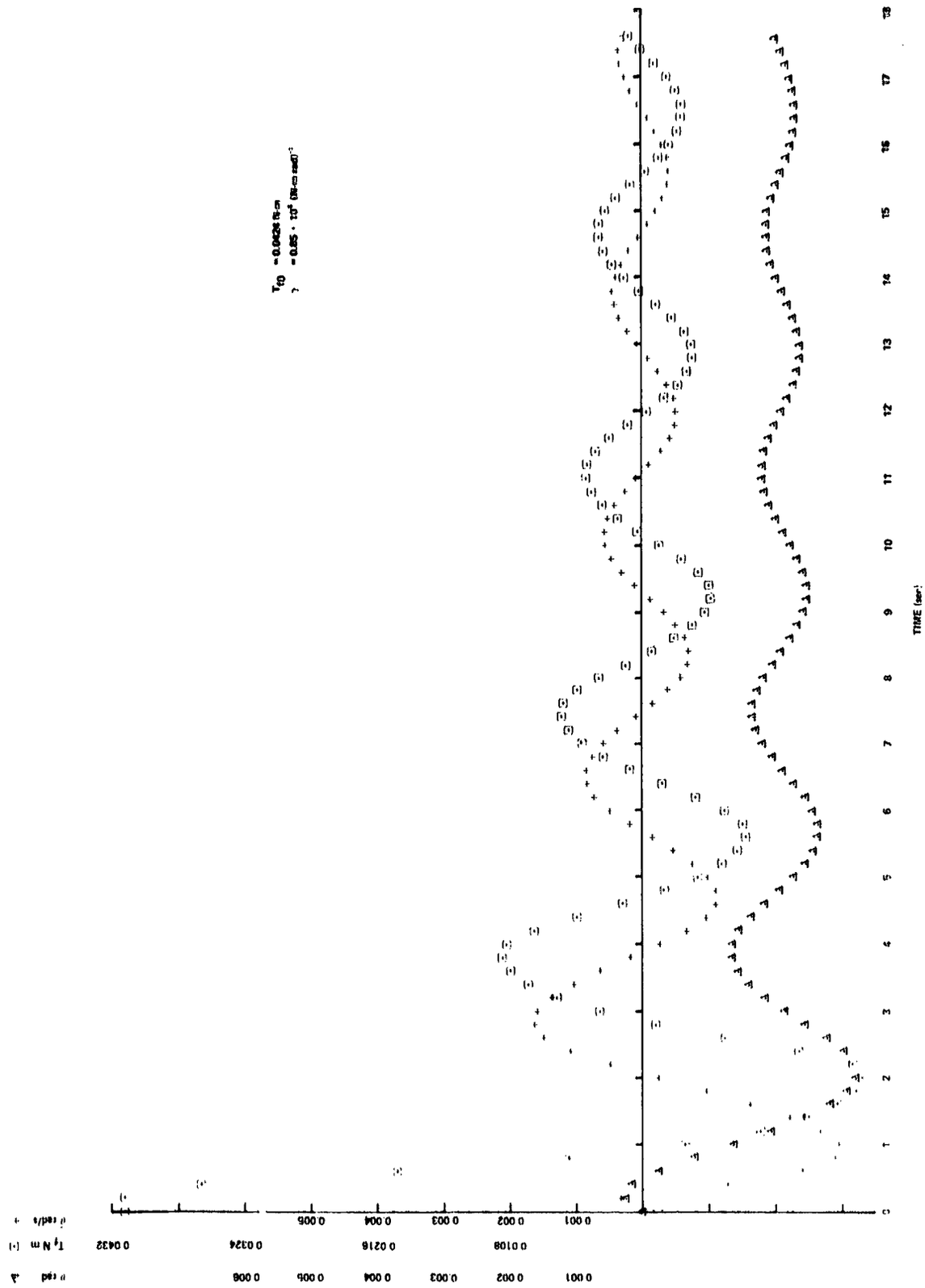

Figure 5. Motion caused by frictional torques.

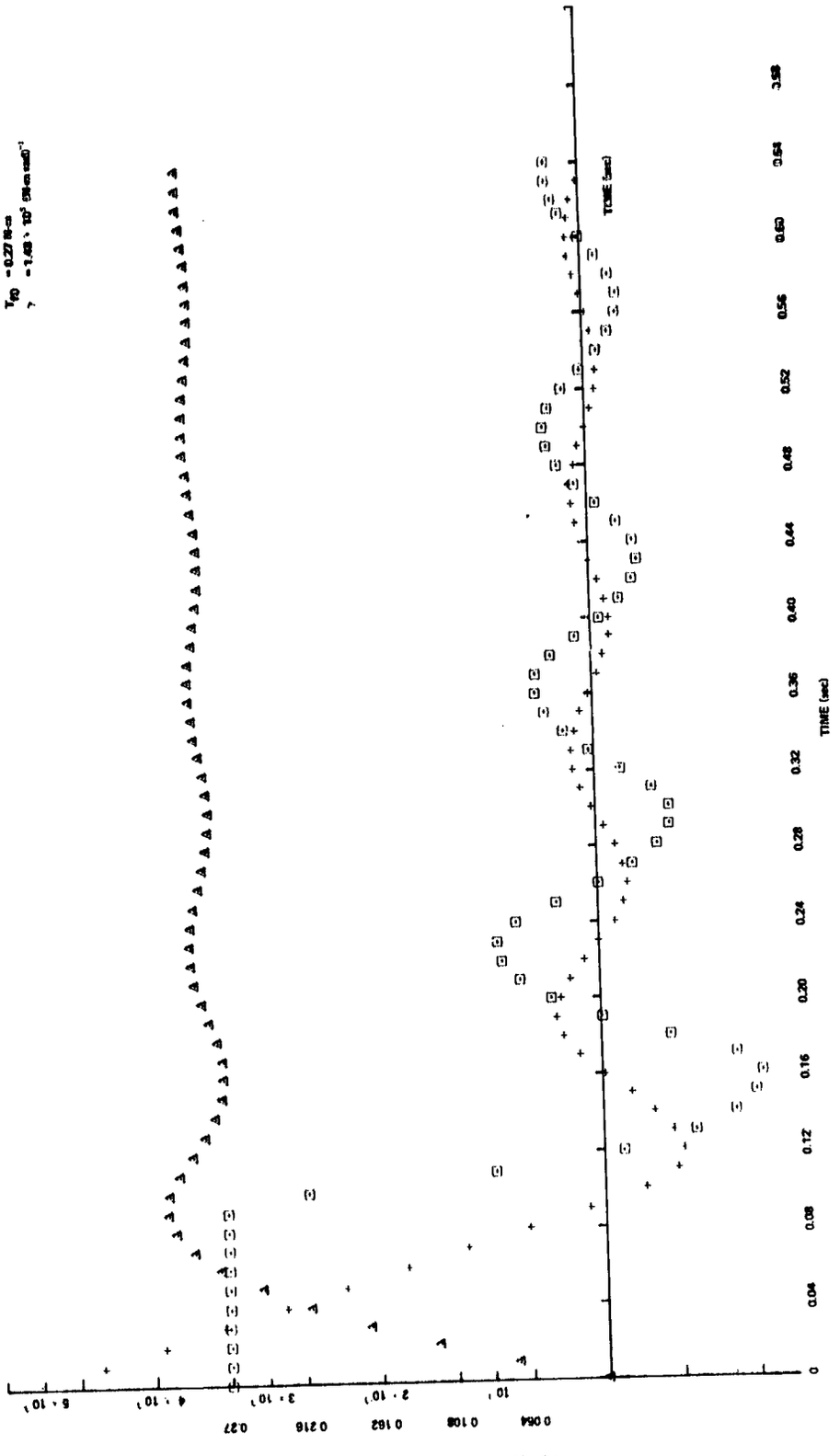

Figure 6. Motion caused by frictional torques.

and

$$\zeta = \frac{K_p}{2\omega_c I} \quad .$$

While the design natural frequency of the control loop depends on the particular application, generally it is above 5 Hz. In Section III it was shown that there was a natural frequency associated with the pivot friction loop given by the equation

$$\omega_f^2 = \frac{\gamma T_{f0}^2}{I} \quad .$$

For the values of γ and T_{f0} in Dahl's report, $\omega_f = 0.28$ Hz as shown in Figure 5. Figure 6, on the other hand, shows that, for the values obtained from a curve fit to CMG data, $\omega_f = 7.4$ Hz. Hence, it is conceivable that ω_f could be similar in magnitude to ω_c. To what extent, then, is such a situation detrimental to the system's performance?

Figures 7 through 10 show the step response for the system defined by equations (10), (11), and (12) for various parameter values. The step commanded gimbal rates, $\dot{\theta}_c$, of 5×10^{-4} rad/s or 5×10^{-5} rad/s are used to show the effect of commanded magnitude on the system response. Figure 11 shows that, for the values of γ and T_{f0} in Dahl's report, the natural frequency of the friction loop, ω_c, and the frictional torque are so small that even for the low level command the friction has very little effect; the response with and without friction are very nearly identical. Figures 8 and 9 show that for $T_{f0} = 0.27$ N-m $\gamma = 1.48 \times 10^5$ [N-m rad]$^{-1}$ the response is affected significantly by the magnitude of $\dot{\theta}_c$ in the range of interest. In the responses of Figures 10 and 11 the control system natural frequency has been increased by a factor of 2, and still there is serious deviation from the desired response.

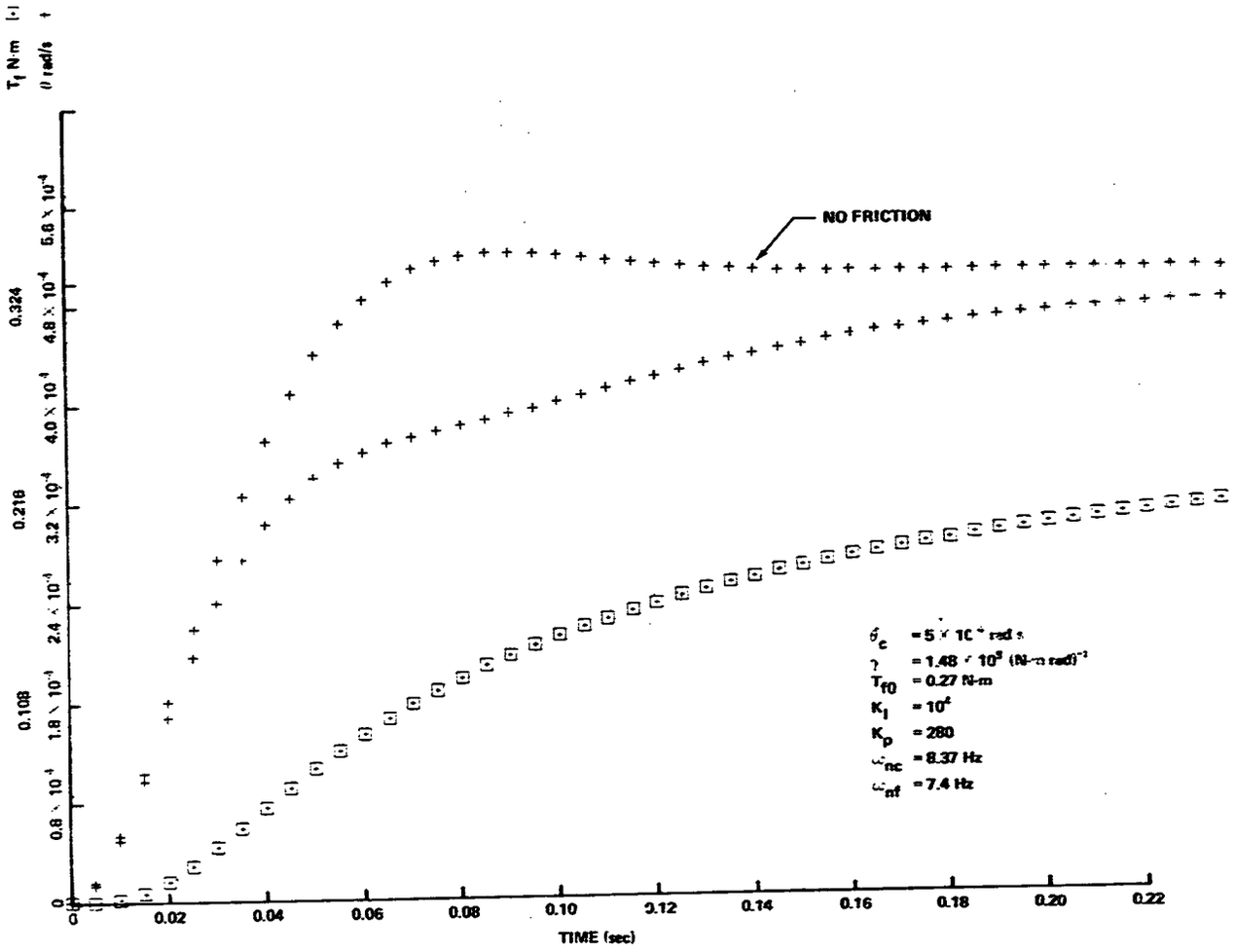

Figure 7. Gimbal rate controller step response.

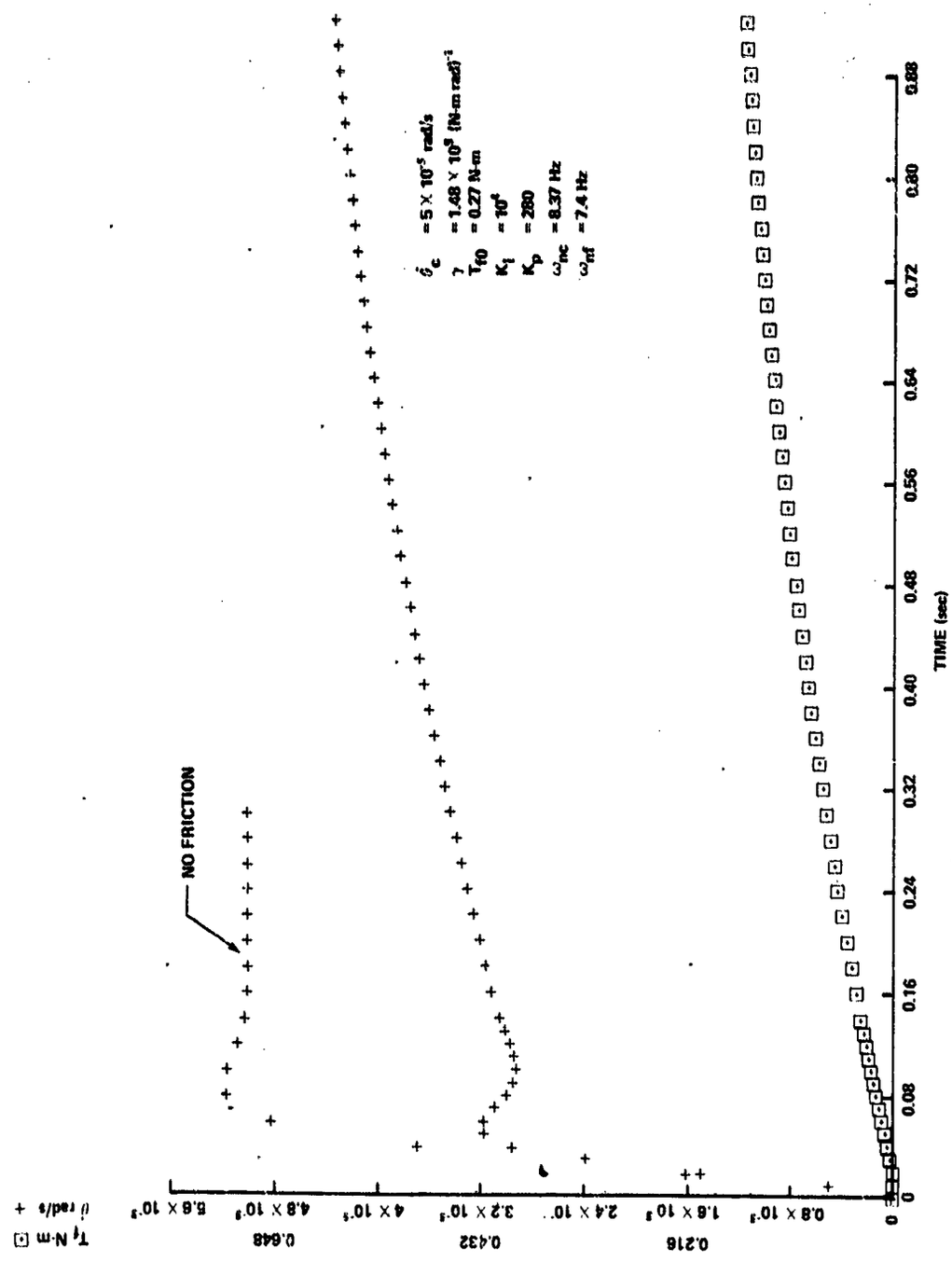

Figure 8. Gimbal rate controller step response.

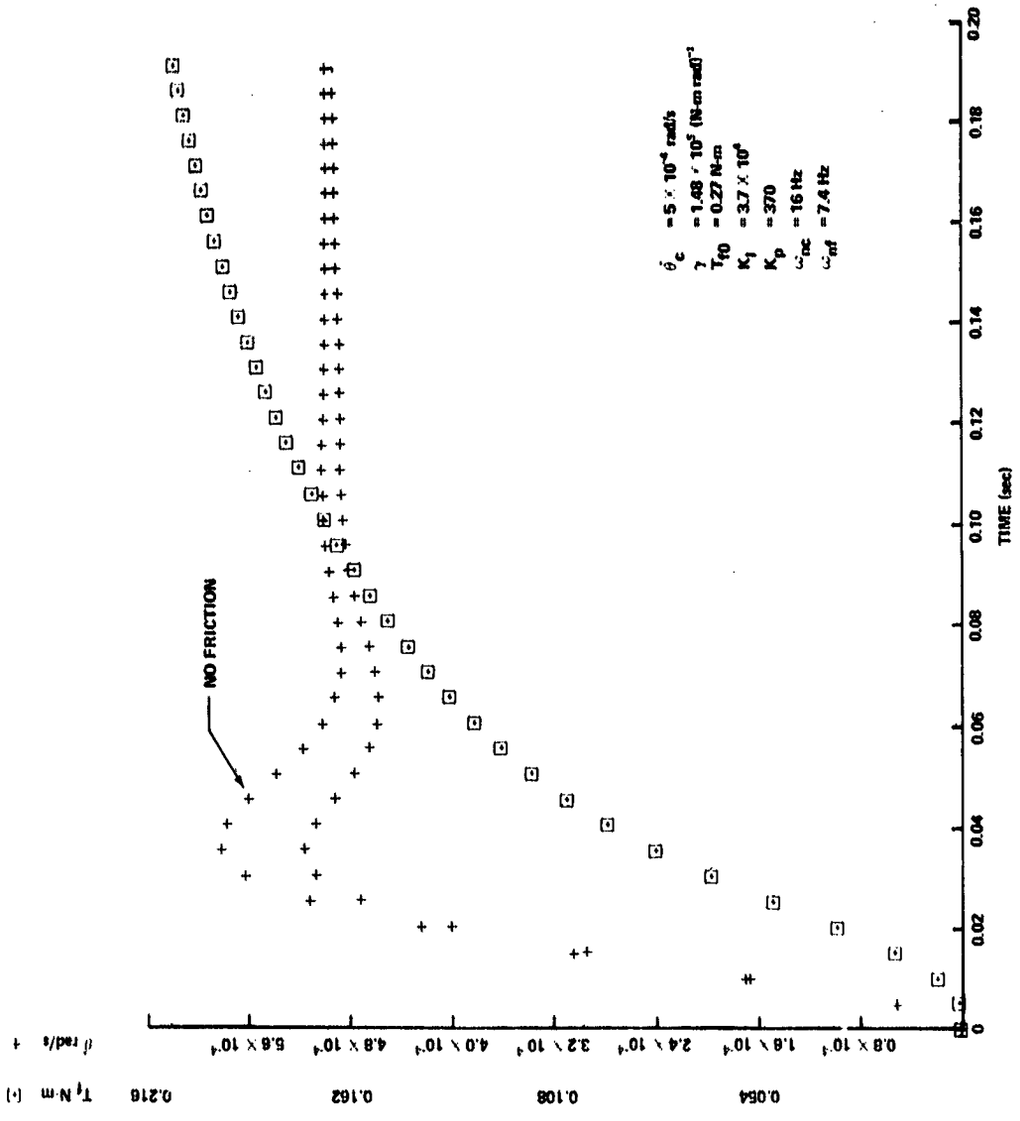

Figure 9. Gimbal rate control

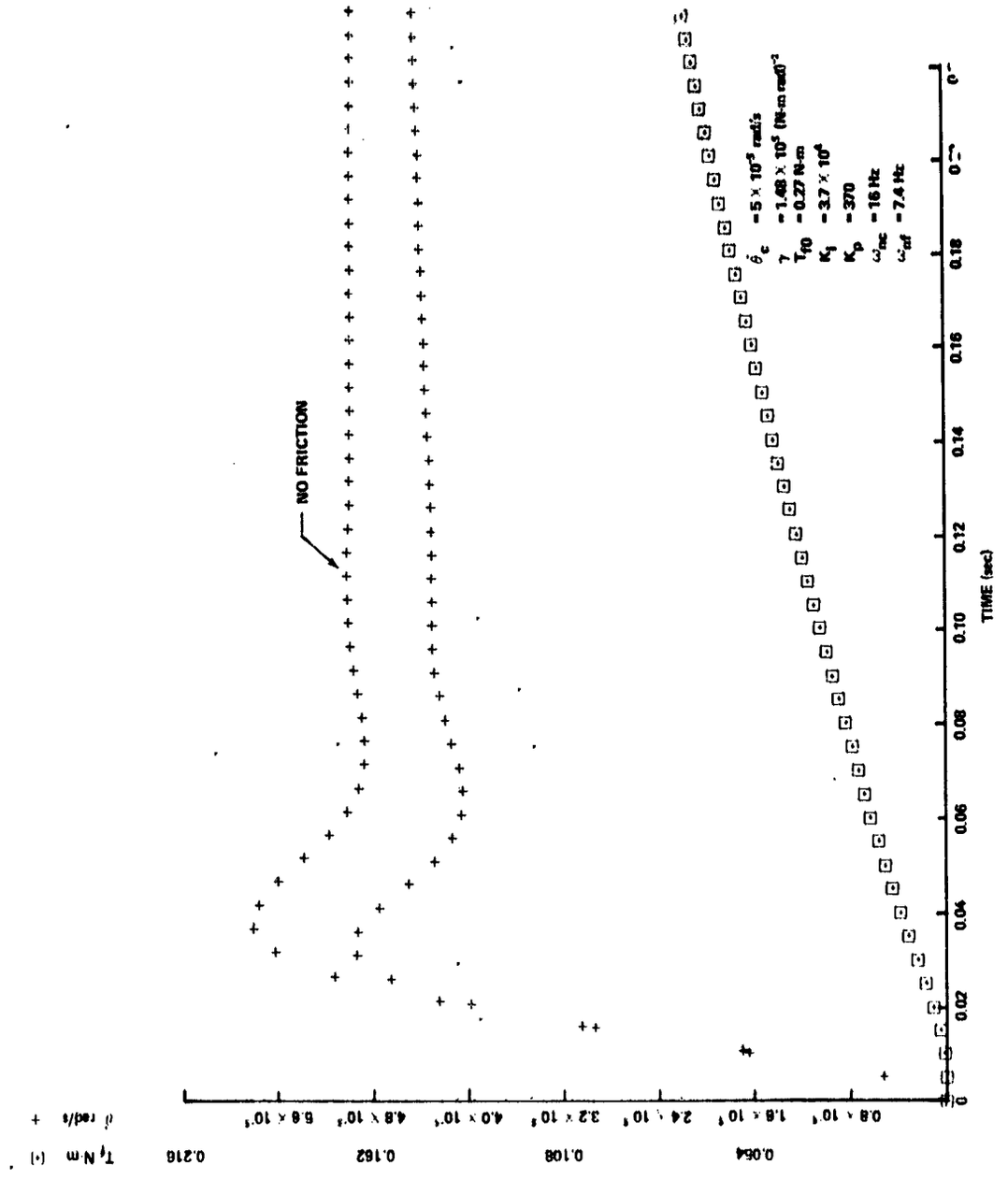

Figure 10. Gimbal rate controller step response.

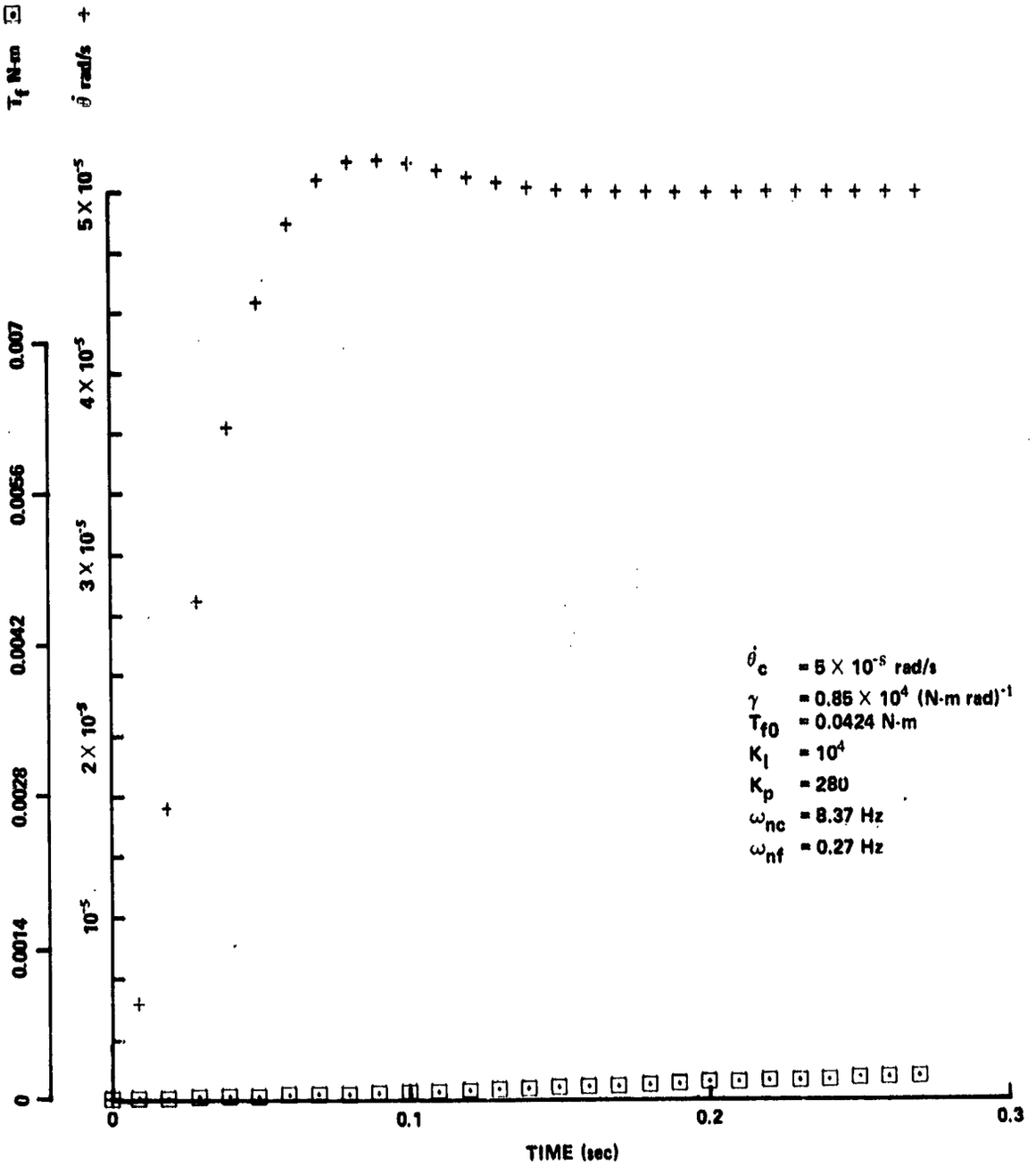

Figure 11. Gimbal rate controller step response.

In Figures 12 through 14 $\dot{\theta}_c$ is a sinusoidal function with a frequency of 2π rad/s. The loss in gain is apparent as the amplitude is decreased.

VI. SUMMARY AND CONCLUSIONS

The basic characteristics of the Dahl friction model have been shown by means of analytical and simulation methods. The effects of friction, represented by the Dahl model, on a CMG gimbal rate control system was investigated by digital simulation. The conclusion from these simulation results is that gimbal pivot friction can have a significant effect on the gimbal rate control system. The magnitude of the problem this presents depends on the characteristics of the actual pivot. It would appear from this preliminary look that one solution is to insure that the control system natural frequency is higher by some prescribed amount than the natural frequency of the friction loop.

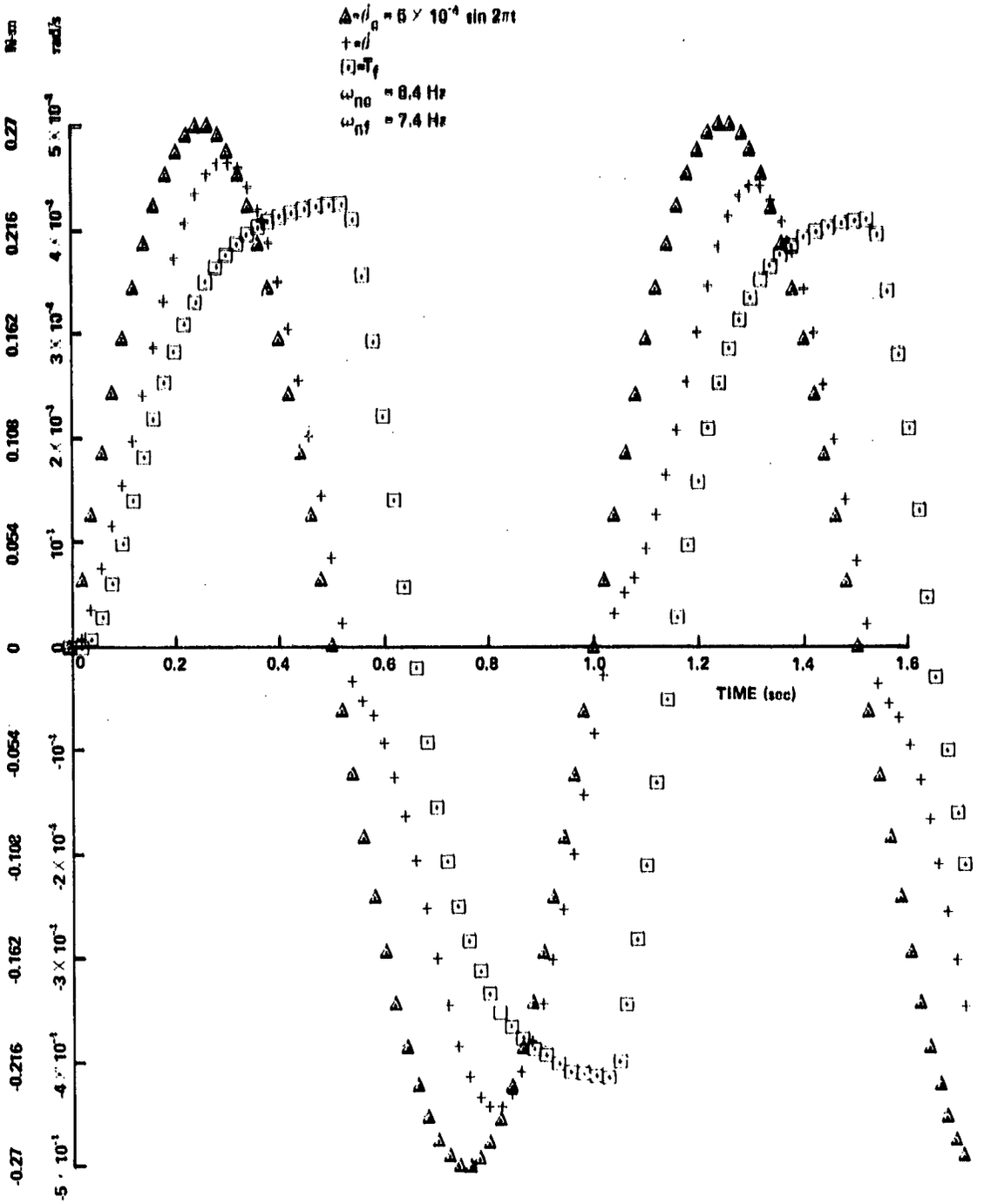

Figure 12. Gimbal rate controller sinusoidal response.

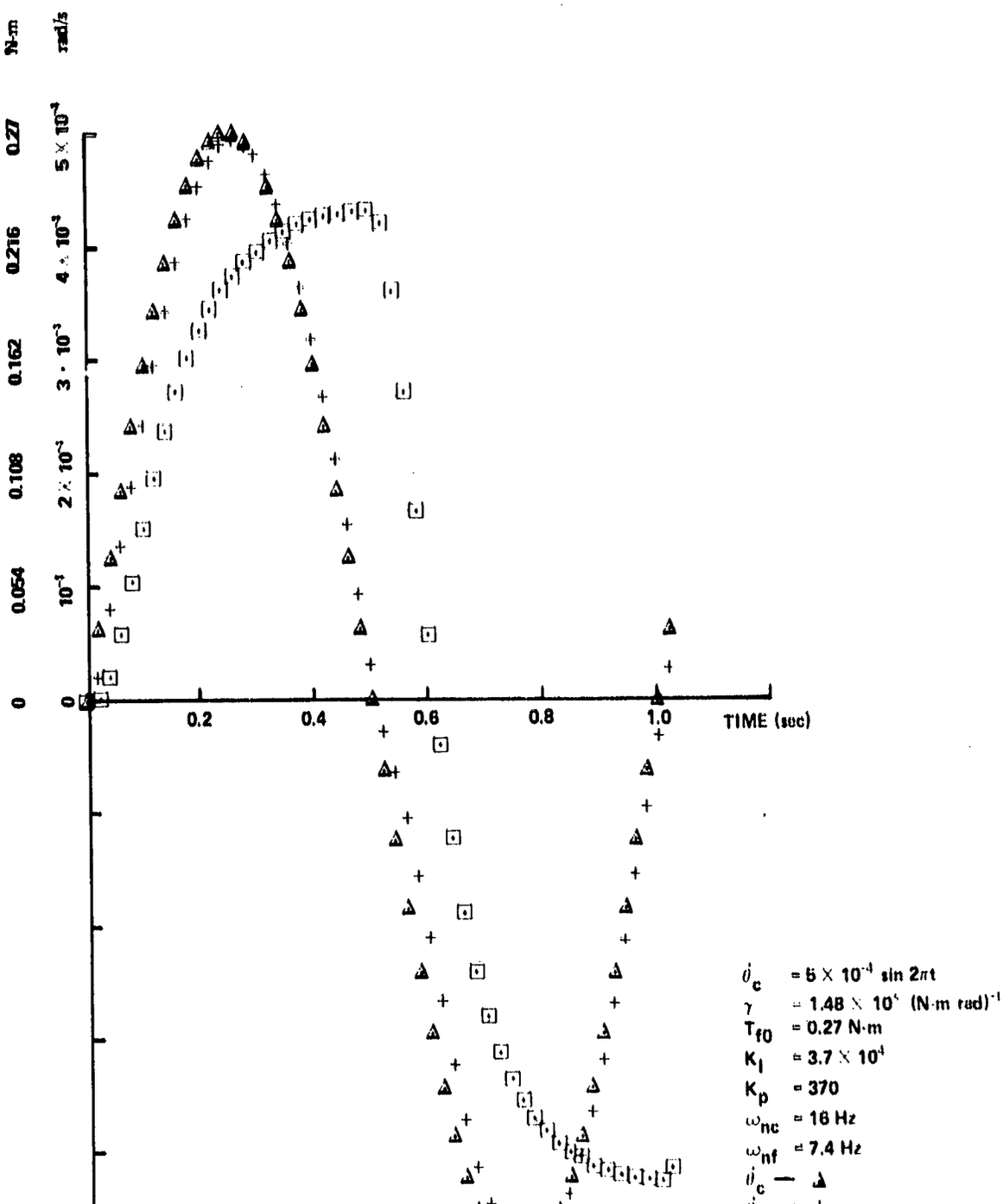

Figure 13. Gimbal rate controller sinusoidal response.

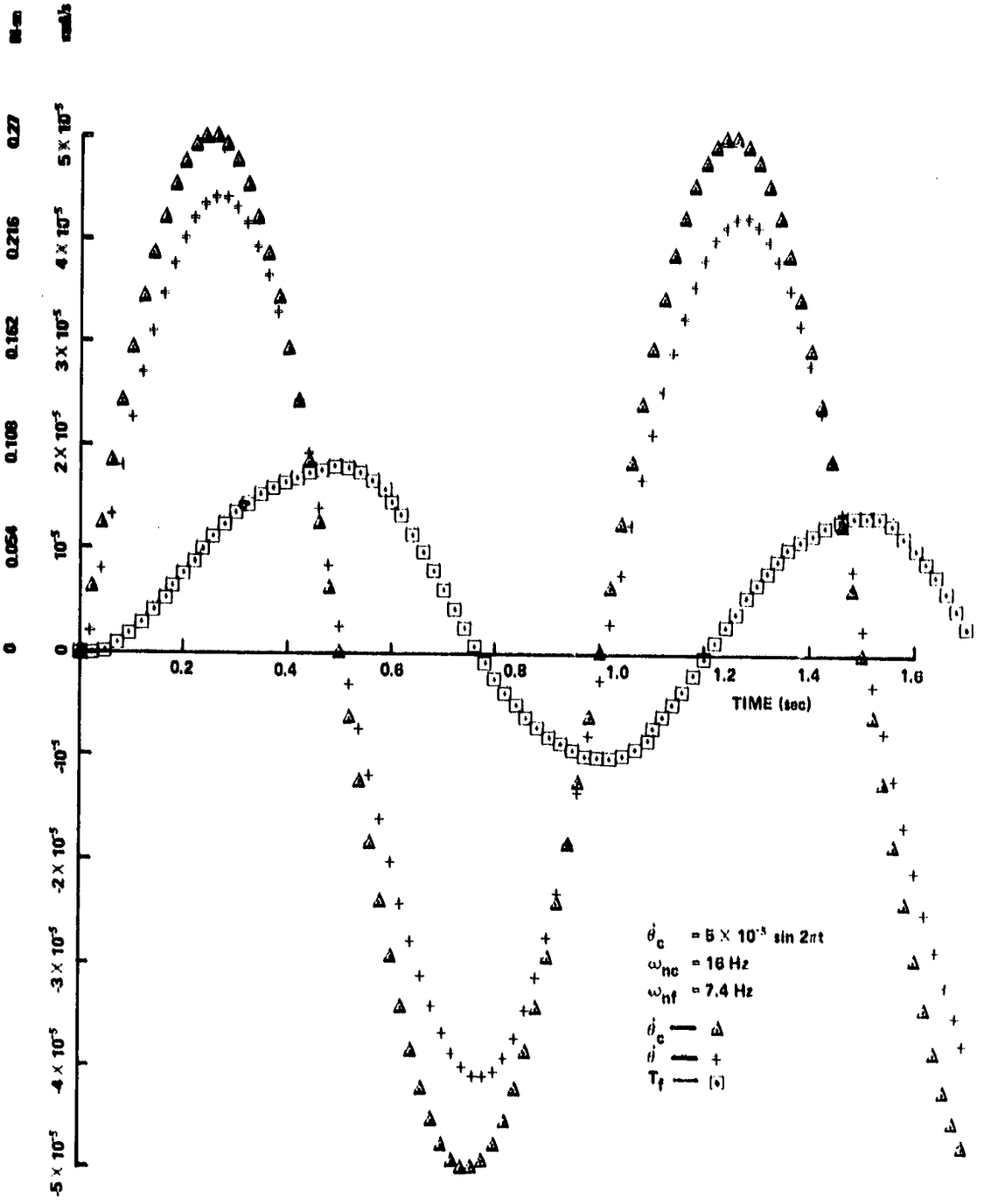

Figure 14. Gimbal rate controller sinusoidal response.

APPROVAL

AN ANALYSIS OF THE DAHL FRICTION MODEL AND ITS EFFECT ON A CMG GIMBAL RATE CONTROLLER

By Gerald S. Nurre

The information in this report has been reviewed for security classification. Review of any information concerning Department of Defense or Atomic Energy Commission programs has been made by the MSFC Security Classification Officer. This report, in its entirety, has been determined to be unclassified.

This document has also been reviewed and approved for technical accuracy.

James C. Blair, Chief
Control Systems Division

J. A. Lovingood, Director
Systems Dynamics Laboratory

☆ U.S. GOVERNMENT PRINTING OFFICE 1976-640-255/295 REGION NO. 4